Acousto-Optic Tunable Filter as a Polychromator and Its Application in Multidimensional Fluorescence Spectrometry

Chieu D. Tran* and Ricardo J. Furlan

Department of Chemistry, Marquette University, Milwaukee, Wisconsin 53233

Acousto-optic tunable filter (AOTF) is an electronically driven dispersive device which operates on the principle of acousto-optic interaction in an anisotropic medium. Incident white light will be diffracted by the AOTF into a specific wavelength when a specific rf is applied to it. The diffracted light needs not be a monochromatic light. Multiwavelength light can be diffracted from the AOTF when several rf signals are simultaneously applied into the filter. Compared to conventional polychromators, advantages of this electronic AOTF polychromator include its ability to individually amplitude-modulate each wavelength of the diffracted multiwavelength light at different frequency. This is accomplished by individually and sinusoidally modulating each applied rf signal at the desired frequency. This feature makes it possible to develop a novel AOTF-based multidimensional fluorimeter in which the sample was simultaneously excited by two different wavelengths (514.5 and 488.0 nm) whose amplitudes were sinusoidally modulated at two different frequencies (100 and 66 Hz). Multicomponent samples, e.g., mixtures of rhodamine 6G and rhodamine B, were successfully analyzed using this novel fluorimeter and the developed data analysis.

INTRODUCTION

Fluorescence technique has been demonstrated to be a sensitive method for trace characterization. Since realtime samples are generally present in multicomponent form, their analyses usually require measurements of the fluorescence spectra at different excitation wavelengths. This time-consuming process was alleviated with the use of the videofluorimeter.[1-5] In this instrument, the monochromators (excitation and emission) are replaced with polychromators. By appropriately configurating the two polychromators and by using a two-dimensional detector such as silicone-intensified target vidicon, emission spectra of the sample produced by the multiwavelength excitation can be simultaneously measured.[1-5] The two-dimensional spectra obtained are then analyzed with the linear algebra techniques.[6,7] The technique has proven to be a very powerful method for the determination of multicomponent trace chemical species. However, in addition to the relatively low sensitivity, the videofluorimeters normally require elaborate data analysis. Novel two-dimensional detectors such as charge-coupled devices (CCDs) and charge-injection devices (CIDs) may provide improvement in the sensitivity but also undesiredly increase the cost.[4] By use of the recently developed acousto-optic tunable filter, a novel and relatively inexpensive multidimensional fluorimeter which has a high sensitivity and simple data analysis can be developed.

Acousto-optic tunable filter (AOTF) is an electronic dispersive device.[8-17] It is based on the acousto-optic interaction in an anisotropic medium. The filter is generally constructed from such birefringent crystal as TeO_2 onto which an array of piezoelectric transducers are bonded. These transducers will transform the applied rf into acoustic wave.[8-17] The propagating acoustic waves produce a periodic moving grating which will diffract portions of an incident beam. Due to the conservation of momentum, only a very narrow band of optical frequencies can be diffracted. Therefore, the spectral bandpass of the filter can be tuned over large optical regions by simply changing the frequency of the applied rf.[8-17] The AOTF is thus similar to the diffraction grating, but in the former, the grating constant, which in this case is the frequency of the acoustic wave, can be electronically changed. Furthermore, since the scanning speed of the AOTF is controlled by the transit time of an acoustic wave across an optical beam which is on the order of few microseconds, the tuning speed of the filter can be as fast as a few microseconds.[8-17] Taken together, compared to other dispersive devices, the AOTF has such advantages as (1) compact, all solid state, rugged, and contains no moving parts; (2) wide angular field; (3) high throughput (diffraction efficiencies of the filter are generally greater than 85%); (4) wide tuning range (from UV through visible to IR); (5) high spectral resolution (bandwidth of light transmitted by the filter is about 2-6 Å); (6) rapid scanning ability (order of few microseconds); (7) light with adjustable intensity; (8) high-speed random or sequential wavelength access; and (9) imaging capability.[8-11] The AOTF has been called "the new generation" monochromator and has offered unique means to develop scientific instruments for fundamental research as well as industrial, medical, and aerospace applications. In fact, advantages of the AOTF have been exploited recently to develop a wide range of instruments which include the fast scanned multiwavelength thermal lens spectrophotometer,[12] the UV, visible and IR absorption, and circular dichroism spectrophotometers,[13-15] the astronomical photometer,[10] the multigas analyzer,[16] and the fluorescence microscope.[17]

In all applications to date the AOTF is used as a fast scanned electronic grating. That is at any given time, only a single

(1) Warner, I. M.; Callis, J. B.; Davidson, E. R.; Gauyeman, M.; Christian, G. D. *Anal. Lett.* **1975**, *8*, 665.
(2) Warner, I. M.; Patonay, G.; Thomas, M. P. *Anal. Chem.* **1985**, *57*, 463A.
(3) Ndou, T. T.; Warner, I. M. *Chem. Rev.* **1991**, *91*, 493.
(4) Warner, I. M.; McGown, L. B. *Advances in Multidimensional Luminescence*; JAI Press, Inc.: Greenwich, CT, 1991.
(5) Vo-Dinh, T. *Room Temperature Phosphorimetry for Chemical Analysis*; John Wiley: New York, 1986.
(6) Warner, I. M.; Callis, J. B.; Christian, G. D.; Davidson, E. R. *Anal. Chem.* **1977**, *49*, 564.
(7) Rossi, T. M.; Warner, I. M. *Appl. Spectrosc.* **1984**, *38*, 422.
(8) Chang, I. C. *Opt. Eng.* **1981**, *20*, 824.
(9) Sivanayayam, a.; Findley, D. *Appl. Opt.* **1984**, *23*, 4601.
(10) Bates, B.; Halliwell, D. R.; McNoble, S.; Li, Y.; Catney, M. *Appl. Opt.* **1987**, *26*, 4783.
(11) Gottlieb, M.; Feichtner, J. D.; Conroy, J. *SPIE International Optical Computing Conference* **1980**, *232*, 33.
(12) Tran, C. D.; Simianu, V. *Anal. Chem.* **1992**, *64*, 1419.
(13) Shipp, W. S.; Biggins, J.; Wade, C. W. *Rev. Sci. Instrum.* **1976**, *47*, 565.
(14) Kradjel, C. *Fresenius' J. Anal. Chem.* **1991**, *339*, 65.
(15) Hatano, M.; Nozawa, T.; Murakami, T.; Yamamoto, T.; Shigehisa, M.; Kimura, S.; Takakuwa, T.; Sakayanagi, N.; Yano, T.; Watanabe, A. *Rev. Sci. Instrum.* **1981**, *52*, 1311.
(16) Nelson, R. L. *ISA Trans.* **1986**, *25*, 31.
(17) Spring, K. R.; Smith, P. D. *J. Microsc.* **1987**, *147*, 265.

0003-2700/92/0364-2775$03.00/0

rf is applied into the filter thereby providing a diffracted beam with only a single wavelength. It is, however, possible to simultaneously apply several rf signals into the filter. This multifrequency application will enable the AOTF to simultaneously diffract more than one wavelength, thereby serving as a polychromator. Optically, this electronic polychromator is relatively easier to use than the conventional grating polychromator because in the former, the diffracted beam is not deviated by the chromaticity of the light, i.e., light with different wavelengths are diffracted from the filter at the same angle. The AOTF is thus particularly suited for the multidimensional fluorimeter. Furthermore, the diffracted light can be made to amplitude modulate at any specific frequency by simply amplitude modulating the applied rf at that same AM frequency. Thus, by AM modulating each applied rf at different AM frequency, each wavelength of the multiwavelength beam diffracted from the AOTF will be AM modulated at a different frequency. When this multiwavelength beam is used to excite the sample, the fluorescence signal will be modulated at those AM frequencies. Therefore, the data analysis will be much simpler and faster than those used in the existing multidimensional fluorimeter. However, in spite of its potentials, AOTF has not been used as a polychromator, and different AM of the AOTF has not been performed. Such consideration prompted us to investigate these possibilities, to implement the AOTF as an electronic polychromator, and to use it to develop a novel, all solid state, fast scanned multidimensional fluorimeter whose data analysis is relatively faster and simpler. Preliminary results on the instrumentation development and its utilization to characterize multicomponent samples will be reported in this paper.

EXPERIMENTAL SECTION

Experiments were designed to investigate the possibility of simultaneously applying many rf signals into the AOTF, to amplitude modulate each rf signal with a different sine wave, and to characterize the light diffracted by the filter for each case. The schematic diagram for the instrument is shown in Figure 1A. A Spectra-Physics argon ion laser (Model 165) operating in the multiline mode was used as the light source. The acousto-optic tunable filter used in this work was the same as previously. Specifically it is a noncollinear type, fabricated from a single crystal of paratellurite (TeO_2) (Matsushita Electronic Components Co., Ltd., Osaka, Japan, Model EFL-F20) and has a clear aperture of 3.0 mm × 5.0 mm. The filter resolution which is defined as the full width at half maximum, $\Delta\lambda$, is given by[8]

$$\Delta\lambda = \frac{\lambda^2}{2l\Delta n \sin^2 \theta_i}$$

where λ is the wavelength of observation, l is the interaction length between the acoustic wave and the light wave, $\Delta n = n_e - n_o$, and θ in the incident angle. The filter is specified to have a resolution of 4 Å at 400 nm.[12] Since Δn, l, and θ are almost constant for the 488.0- and 514.5-nm wavelengths, the resolutions for these two wavelengths were calculated to be 6.0 and 6.6 Å, respectively. However, the difference of 0.6 Å in the resolution at the two wavelengths used should not affect the results of the present work because these two wavelengths, being derived from the argon ion laser, are monochromatic.

Two different oscillators (Osc 1 and Osc 2, MCM Electronics, Centerville, OH, Model TENMAC 72-585) were used to provide two different rf signals. These rf signals were sinusoidally amplitude modulated at two different frequencies (66 and 100 Hz) by two home-built modulators (Mod 1 and Mod 2) whose circuitries are shown in Figure 1B. Essentially, the rf signal provided by the oscillator was amplified by an amplifier (A, Mini-Circuits, Brooklyn, NY, Monolithic Amplifier MAV-11) prior to being modulated by a Mini-Circuits Model CBL-1 mixer. The modulation signal which was provided by a microcomputer (IBM AT compatible with a 386 microprocessor (Northgate Computer

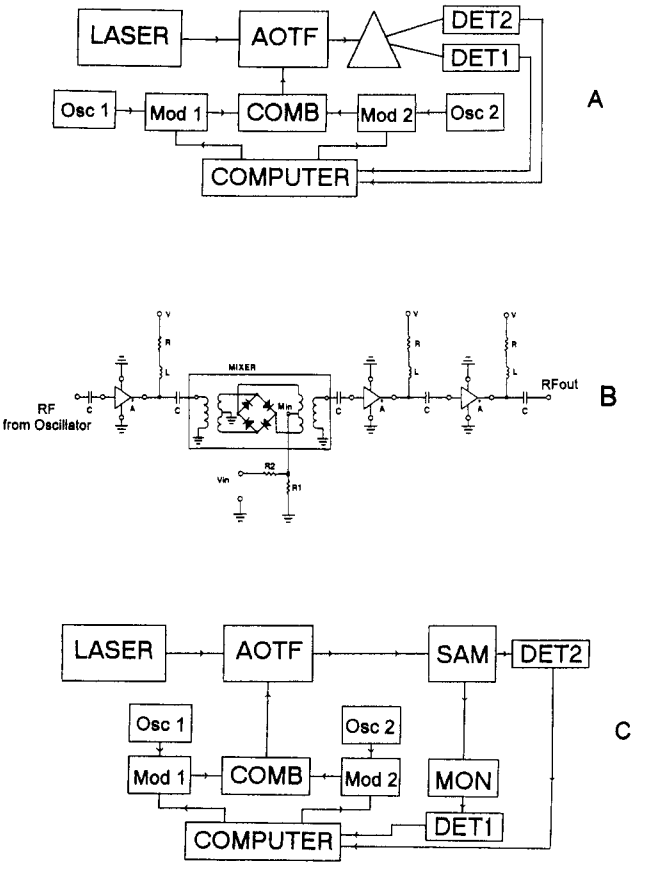

Figure 1. (A) Schematic diagram of the apparatus to characterize the light diffracted by the AOTF: AOTF, acousto-optic tunable filter; DET1 and DET2, PIN photodiode; Osc 1 and Osc 2, oscillator to provide the rf signal; Mod 1 and Mod 2, modulator to sinusoidally amplitude-modulate the rf signals; COMB, rf combiner; SAM, sample. (B) The circuitry to modulate and amplify the rf signal: C, 2200 pF capacitor; L, 1.2 μH inductor; R, R1 and R2, 100-Ω × 1/2-W, 50-Ω × 1/4-W, and 680-Ω × 1/4-W resistors; V, 11.6 V; A, Mini-Circuit MAV-11 monolithic amplifier and MIXER, Mini-Circuit CBL-1 mixer. (C) The apparatus to measure fluorescence: MON, monochromator; DET1, photomultiplier tube; DET2, PIN photodiode; other symbols are the same as in A.

Systems, Eden Prairie, MN)) through the D/A of the 12-bit DAS 16 board (Metra-Byte, Taunton, MA). The power of each modulated rf signal at this point was not adequate to drive the AOTF. Therefore, they were consecutively amplified by two amplifiers (A) to achieve a maximum power level of 20 dBm. Subsequently they were combined by means of a combiner (COMB, Mini-Circuits splitter/combiner Model ZSC-2-1) before being connected to the AOTF.

When the AOTF was applied by the signal which contains two different rf's, the diffracted light had two different wavelengths. This dual-wavelength light was dispersed into individual colors by an equilateral prism (Figure 1A). The intensities of each beam are measured by a PIN photodiode (DET1 and DET2, United Detector Technology Model 10DP).

Subsequent to the confirmation of this multifrequency diffraction and the characterization of the diffracted light, the instrument was modified for the fluorescence measurements. The set up is shown in Figure 1C. As illustrated, the sample (SAM) was excited by the sinusoidally modulated diffracted light. The fluorescence emitted was dispersed by the monochromator (Oriel model 7240) and detected by a photomultiplier tube (DET 1, Hamamatsu Model R446). A PIN photodiode (DET 2, United Detector Technology Model 10 DP) was used to measure the light transmitted through the sample for reference.

A computer program was written to provide sinusoidal amplitude modulations for the rf signals and to acquire and to analyze data. Through one A/D-D/A board (DAS-16), one subroutines of the program was developed to send the sinusoidal signals (through the D/A) to separately amplitude modulate each of the rf signals at a different AM frequency, and to acquire the

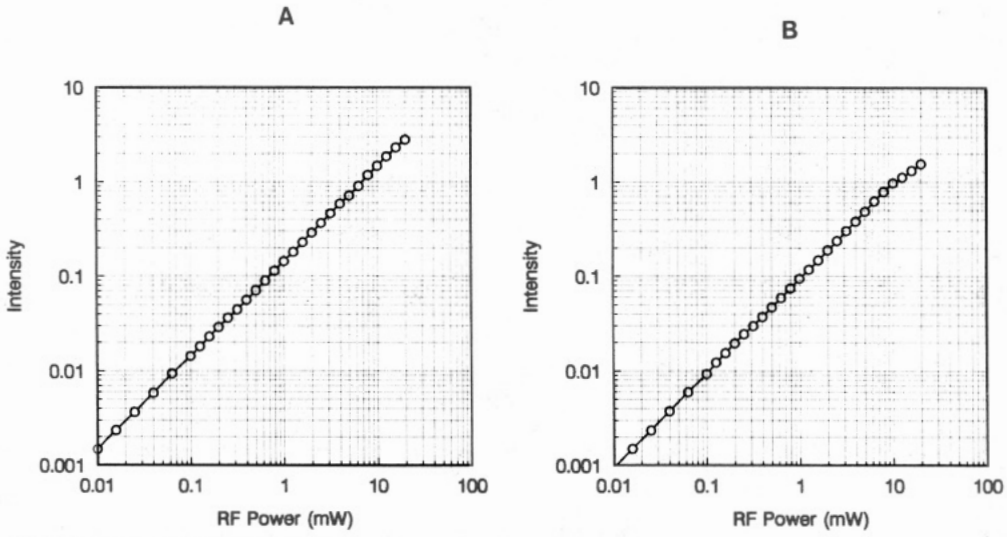

Figure 2. Relationship between the power of the applied rf and the intensity of the diffracted light for 514.5-nm beam (A) and 488.0-nm beam (B).

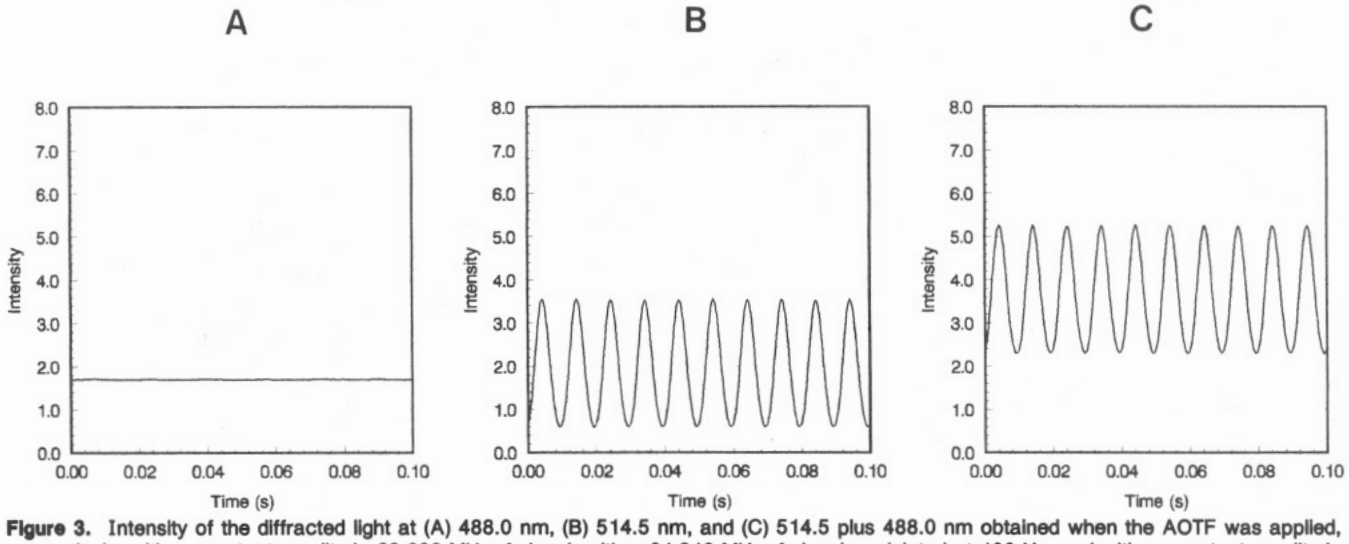

Figure 3. Intensity of the diffracted light at (A) 488.0 nm, (B) 514.5 nm, and (C) 514.5 plus 488.0 nm obtained when the AOTF was applied, respectively, with a constant-amplitude 69.200-MHz rf signal, with a 64.310-MHz rf signal modulated at 100 Hz, and with a constant-amplitude 69.200-MHz rf plus the 64.310-MHz signal modulated at 100 Hz.

data (through the A/D). The data collected was analyzed by a program whose main function is to calculate the averages of the excitation and fluorescence signals (i.e., AV_I and AV_F in eq 17 and 19 of the Appendix). Through signals summation, the program also enables the calculation of the frequency components of the excitation and fluorescence signals (i.e., Q_{I_n} in Q_{F_n} in eqs 18 and 20 of the Appendix).

RESULTS AND DISCUSSION

1. Acousto-Optic Tunable Filter as a Polychromator. The two wavelengths used in this work are 514.5 and 488.0 nm. They were obtained by applying rf frequencies of 64.310 and 69.200 MHz, respectively, to the AOTF. Initial investigation was on the relationship between the power of the applied rf and the intensity of the diffracted light. As shown in Figure 2A,B, the intensities of the 514.5- and 488.0-nm light are linearly proportional to the power of the applied rf for over four decades of power.

It was found that the AOTF will diffract light having two different wavelengths when two different rf signals are simultaneously applied into it. For example the filter will diffract light at 514.5 nm when an rf signal of 64.310 MHz is applied into it. Changing the frequency to 69.200 MHz led to the change in the wavelength to 488.0 nm. When both frequencies, 64.310 and 69.200 MHz, were simultaneously applied into the filter, the intensity of the diffracted light, as measured by the detector 2 (DET2) of the set up shown in Figure 1C, is the sum of the intensities of the 514.5-nm light and of the 488.0-nm light. To further confirm this observation, the diffracted light was dispersed by a prism using the apparatus shown in Figure 1A. It was found that the diffracted light contained two wavelengths, 514.5 and 488.0 nm, whose intensities as measured by DET1 and DET2 (of the instrument shown in Figure 1A) were the same as the intensities obtained when the filter was individually applied at a frequency of 64.310 or 69.200 MHz. It is thus evidently clear that when applied by an rf signal of multifrequencies, the AOTF will diffract multicolor light. Each color component of the diffracted light corresponds to each frequency of the applied rf. There was no interaction between one color component and others.

Subsequently, the response of the AOTF when it is applied by a sinusoidally modulated rf signal was investigated. Figure 3A shows the intensity of the 488.0-nm diffracted light when the AOTF was applied by an rf frequency of 69.200 MHz. Changing the frequency of the applied rf to 64.310 MHz and amplitude modulating it by a sinusoidal signal at 100 Hz resulted in the sinusoidal modulation of the diffracted light at the same frequency of 100 Hz (Figure 3B). When the two rf signals (i.e., the constant-amplitude rf at 69.200 MHz and

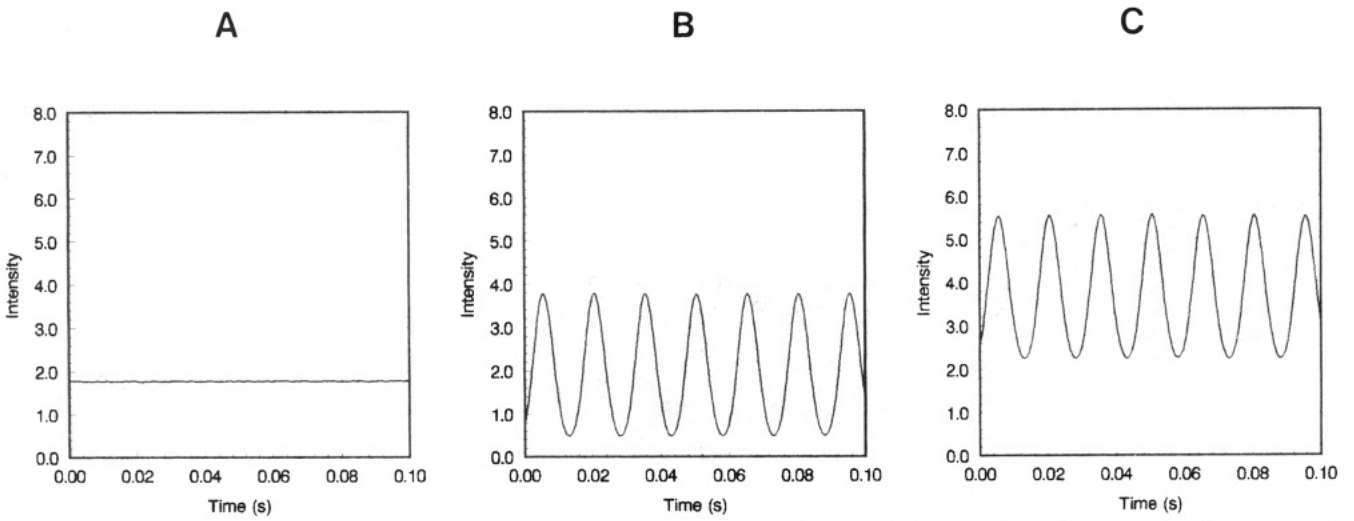

Figure 4. Intensities of the diffracted light at (A) 514.5 nm, (B) 488.0 nm, and (C) 514.5 plus 488.0 nm obtained when the AOTF was applied, respectively, with a constant-amplitude 64.310-MHz signal plus the 69.200-MHz signal modulated at 66 Hz.

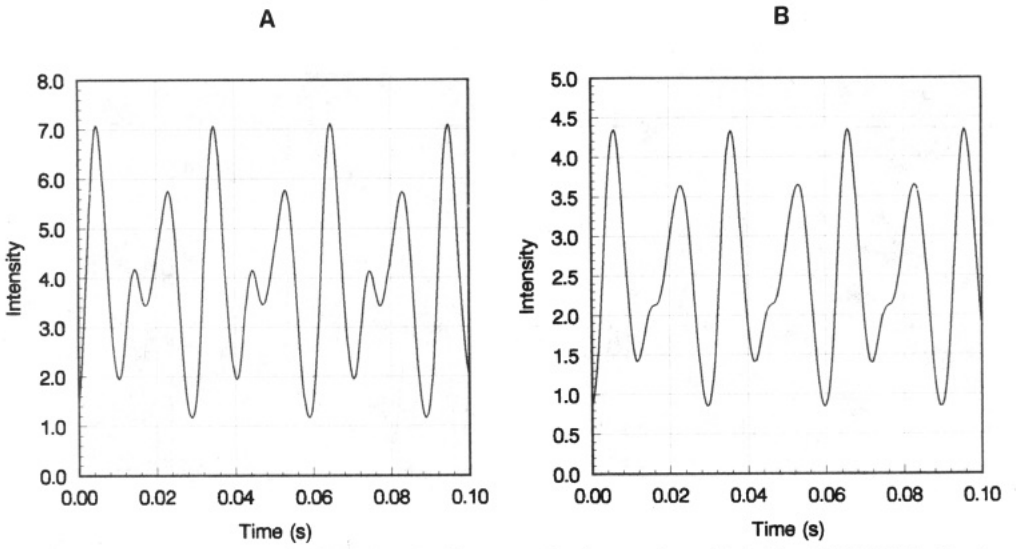

Figure 5. (A) Intensity of the light diffracted by the AOTF when the filter was simultaneously applied with a 64.310-MHz signal modulated at 100 Hz and 69.200-MHz signal modulated at 66 Hz. (B) Fluorescence intensity (at 517 mm) of a 9.88×10^{-8} M solution of fluorescein in methanol when it was excited by the light shown in A.

the sinusoidal-modulated rf at 64.310 MHz) were simultaneously applied into the AOTF, the amplitude of the diffracted light was sinusoidally modulated at 100 Hz (Figure 3C). When spectrally dispersed by a prism using the apparatus shown in Figure 1A, it was found that this diffracted beam contains two different wavelengths, 488.0 and 514.5 nm. As revealed by detectors 1 and 2 (i.e., DET1 and DET2 in Figure 1A), the 488.0-nm beam had a constant amplitude and the same intensity as the one shown in Figure 3A. The amplitude of the 514.5-nm beam was sinusoidally modulated at 100 Hz and was the same as the one previously shown in Figure 3B. Conversely, when the AOTF was simultaneously applied by two rf signals: a constant-amplitude 64.310 MHz and the sinusoidally-modulated (at 66 Hz) 69.200 MHz, the diffracted light (Figure 4C) was a combination of two different wavelengths 514.5 and 488.0 nm. The 514.5-nm beam as shown in Figure 4A had a constant amplitude whereas the 488.0-nm beam was amplitude modulated at 66 Hz (Figure 4B). When the two applied rf signals (69.200 and 64.310 MHz) were sinusoidally modulated (at 100 and 66 Hz, respectively) the diffracted light, as shown in Figure 5A, is a mixture of the two sinusoidally modulated 514.5- and 488.0-nm beams (i.e., Figures 3B and 5B). These results clearly demonstrate that by sinusoidally modulating the amplitude of the applied rf signal, the diffracted light will be sinusoidally modulated at the same frequency. The diffracted light depends only on the nature of the corresponding rf signal. It will be AM modulated at the same frequency of the amplitude modulation of the applied rf. When the applied signal was a mixture of more than one sinusoidally modulated rf's, there was no influence on one wavelength component of the diffracted light by the AM modulations of other rf signals which are not correspondent to this particular wavelength. In other words, there was no interaction or "cross talk" between the AM modulation of one rf and the others.

To illustrate the absence of cross talk and the validity of the theory and data analysis, additional experiments were performed in which different combinations and modulation indices of the sinusoidal amplitude modulations were used. The results are listed in Table I. In all of the cases listed in Table I, the AOTF was simultaneously applied by two different rf's: 64.310 and 69.200 MHz. Using the apparatus shown in Figure 1A, the diffracted light was spectrally resolved into two wavelengths, 514.5 and 488.0, whose intensities were detected by detector 1 and 2 (DET1 and DET2), respectively. The output signals of the detectors were fed into the computer for data analysis using methods described in the theory and experimental section. As listed in Table I, in case 1, the AOTF was simultaneously applied with two rf's, 64.310 and 69.200 MHz. The amplitude of the 69.200-MHz signal was kept

Table I. Types of the Applied rf Signals and Properties of Light Diffracted from the AOTF

	amplitude of sinusoidal modulation		intensity					
			detector 1			detector 2		
				modulated component			modulated component	
case	514.5 nm (100 Hz)	488.0 nm (66 Hz)	average	100 Hz	66 Hz	average	100 Hz	66 Hz
1	1.00	0.00	3.524	1.960	0.000	2.162	0.000	0.000
2	0.75	0.00	3.120	1.484	0.000	2.162	0.000	0.000
3	0.50	0.00	2.822	0.994	0.000	2.159	0.000	0.000
4	0.25	0.00	2.646	0.499	0.000	2.159	0.000	0.000
5	0.00	0.00	2.593	0.000	0.000	2.159	0.000	0.000
6	0.00	1.00	2.583	0.000	0.000	3.011	0.000	1.836
7	0.00	0.75	2.590	0.000	0.000	2.642	0.000	1.391
8	0.00	0.50	2.580	0.000	0.000	2.372	0.000	0.933
9	0.00	0.25	2.587	0.000	0.000	2.215	0.000	0.470
10	0.00	0.00	2.593	0.000	0.000	2.159	0.000	0.000
11	1.00	1.00	3.539	1.969	0.000	3.020	0.000	1.841
12	1.00	0.75	3.538	1.968	0.000	2.652	0.000	1.396
13	0.50	1.00	2.823	0.994	0.000	3.017	0.000	1.839
14	0.25	0.75	2.646	0.499	0.000	2.645	0.000	1.393
15	0.00	0.00	2.593	0.000	0.000	2.159	0.000	0.000

constant while the 64.310-MHz signal was sinusoidally modulated at 100 Hz (at the modulation level of 1.00). The output signal of the detector 1 which detected the 514.5-nm beam was analyzed for the average component of the signal (i.e., AV_I in eq 17 of the Appendix). The modulated components of the signal at 100 and at 66 Hz (i.e., Q_I in eq 18 of the Appendix) were also analyzed. Similarly, the signal output of detector 2 which detected the 488.0-nm beam was analyzed for the average, and the modulated components at 100 and at 66 Hz. As expected, in this case, only the intensity of the light at 514.5 nm was modulated (at 100 Hz) because the sinusoidal modulation was applied to the 64.310-MHz signal. The 488.0-nm light was not detected at the detector 1. At the detector 2, which detected the 488.0-nm beam, only a constant light intensity was detected. No modulation at either 100 or 66 Hz was observed at this detector. As expected from eq 18, decreasing the AM modulation index (i.e., m) by 25% (case 2), 50% (case 3), and 75% (case 4) led to 24.3%, 49.3%, and 74.5% decreases, respectively, in the modulation component of the 514.5-nm beam at 100 Hz. There was no change in the average intensity of the 488.0-nm beam as detected by detector 2. In cases 6–9, the amplitude of the 64.310-MHz signal was kept constant while the 69.200-MHz signal was sinusoidally modulated at 66 Hz (at different magnitudes, i.e., different m values). As expected, detector 1 detected only a constant magnitude signal at 514.5 nm. There were no modulated components at either 100 or 66 Hz at this detector. Conversely, detector 2, which detected the 488.0-nm beam, detected the signal which was modulated at 66 Hz. There was no modulation of this 488.0-nm signal at 100 Hz. The magnitude of the 66-Hz-modulated 488.0-nm signal was decreased to 75.8%, 50.8%, and 25.6% of the 100% modulation value (i.e., 1.836 in case 6) as the modulation index decreased to 75% (case 7), 50% (case 8), and 25% (case 9), respectively. In cases 11–14, both rf signals were sinusoidally modulated. The 64.310-MHz signal was modulated at 100 Hz while the 69.200-MHz signal was modulated at 66 Hz. As expected, the 514.5-nm beam was modulated only at 100 Hz, not at 66 Hz (detector 1) whereas the 488.0-nm beam was modulated only at 66 Hz (detector 2). Decreasing the modulation index of the 514.5- and 488.0-nm beam by 75% and 25%, respectively (case 14), resulted in the decrease in the magnitudes of the modulated signals at 100 Hz (for the 514.5-nm beam) and at 66 Hz (for the 488.0-nm beam) by 74.7% and 24.3%, respectively. Only constant 514.5- and 488.0-nm beams were detected where neither the 64.310- nor the 69.200-MHz signals were sinusoidally modulated (case 15).

Collectively we have successfully demonstrated that the AOTF can be used as a polychromator, i.e., the filter can simultaneously diffract more than one wavelength at the same time. Compared to the conventional gratings, the AOTF, in addition to its inherent advantages such as all solid state, compact, fast scanning capability, and containing no moving parts, can also provide some unique features, namely the multiwavelength beam diffracted from the filter is well collimated (i.e., all wavelengths will be diffracted from the filter at approximately the same angle). Furthermore, by amplitude modulating each applied rf signal at different frequency, each wavelength of the diffracted multiwavelength beam will be modulated at different frequency. It should be noted that in this study the laser was used as a light source. However, the AOTF is not limited to this type of light source. Due to the relatively large acceptance angle, the AOTF can be utilized with other light sources which do not provide well-collimated beams, e.g., incandescent and arc lamp. These features enable the AOTF to serve as a unique means in the development of novel instruments. In the following section, the AOTF is used as a novel polychromator to construct a novel multidimensional fluorescence spectrophotometer. The instrumentation development and preliminary results will be described.

2. Multidimensional Fluorescence Spectrophotometer Based on the AOTF. Fluorescence signals of 9.88×10^{-8} M solution of fluorescein in ethanol were measured at 517 nm using the apparatus shown in Figure 1C. It was found that there was no modulation in the fluorescence signal of the sample when it was excited by a constant-amplitude (no modulation) 514.5-nm beam (i.e., the beam whose intensity was shown previously in Figure 4A). The lack of the modulated component is further confirmed when the fluorescence signal was analyzed, according to the method described in the previous section, to calculate the average (i.e., AV_F) and modulated components (Q_F). The analyzed results were listed in Table II. As listed, the fluorescence signal belongs to case 1 where there was no modulation in the fluorescence signal at either 66 or 100 Hz; the constant (i.e., average) is the only component in the signal. When the sample was excited by the 488.0-nm beam sinusoidally modulated at 66 Hz (whose intensity profile was shown previously in Figure 4B), the fluorescence signal seems to modulate at the same frequency. This is case 5 and as the calculated results illustrate, the fluorescence signal does, in fact, modulate at 66 Hz. When both of these excitation beams were simultaneously applied into the sample, the fluorescence signal obtained is expected to be the combination of the two previous

Table II. Fluorescence Intensities (at 517.0 nm) of a 9.88×10^{-8} M Solution of Fluorescein in Ethanol

	excitation light		fluorescence		
				modulated component	
case	514.5 nm	488.0 nm	average	100 Hz	66 Hz
1	on, no modulation	off	0.835	0.000	0.000
2	off	on, no modulation	1.363	0.000	0.000
3	on, no modulation	on, no modulation	2.228	0.000	0.000
4	on, modulated at 100 Hz	off	0.905	0.294	0.000
5	off	on, modulated at 66 Hz	1.560	0.000	0.616
6	on, modulated at 100 Hz	on, no modulation	2.308	0.306	0.000
7	on, no modulation	on, modulated at 66 Hz	2.391	0.000	0.617
8	on, modulated at 100 Hz	on, modulated at 66 Hz	2.475	0.302	0.616

signals. The analyzed results (case 7) show that this is, in fact, the case. That is the average component of the signal (2.391) is the sum of the average component of 0.835 in case 1 and 1.560 in case 5. The signal is expectedly modulated at 66 Hz and its modulated component at this frequency (0.617) is the same as that of case 5 (0.616). Similar results were obtained when the sample was excited by a constant-amplitude 488.0-nm beam (case 2); by the 514.5-nm beam modulated at 100 Hz (case 4), and by the combination of both of these beams (case 6). Figure 5B and case 8 illustrate the fluorescence signal of the sample when it was simultaneously excited by the modulated (at 100 Hz) 514.5-nm beam and the modulated (at 66 Hz) 488.0-nm beam (the intensity profile of this combined excitation beam was shown in Figure 5A). The calculated signal shows that, as expected, the average component (2.475) is, within experimental error, the sum of the individual cases (i.e., 0.905 in case 4 and 1.560 in case 5). The fluorescence signal is modulated at 100 Hz as well as at 66 Hz. However, the 100-Hz modulation is due to the 100-Hz 514.5-nm excitation beam (i.e., compare the 0.302 in case 8 and 0.306 in case 6) and the 66-Hz 488.0-nm beam is responsible for the 66-Hz modulation component in the signal (0.616 in case 8 and 0.616 in case 5). There was no cross talk between the modulation of one beam and the fluorescence induced by the other beam.

Taken together, the results obtained provide a clear and unequivocal evidence for the fact that the AOTF-based fluorimeter is capable of simultaneously measuring fluorescence signals at two different wavelengths and for the validity of the derived theory and data analysis. Subsequently, the instrument was used for the determination of one- and two-component samples. Three different dyes, namely fluorescein, rhodamine 6G, and rhodamine B, were selected for this preliminary study. For fluorescein, calibration curves at two different wavelengths, 514.5 and 488.0 nm, were constructed from the measured fluorescence signals using the (calculated) modulated components at 514.5 nm (100 Hz) and at 488.0 nm (66 Hz). Linear relationship (not shown) was obtained for both wavelengths (correlation coefficients are 0.9986 and 0.9987, respectively) for the concentrations range from 9.88×10^{-9} to 7.41×10^{-7} M.

Simultaneous determination of concentrations of each component in the two-component mixture was then performed using this AOTF-based fluorimeter. Rhodamine B and rhodamine 6G were the two dyes selected for this determination. Individually, these two dyes exhibit a linear relationship between the concentration and the fluorescence intensity detected at 563 nm and excited at 514.5 and 488.0 nm. Correlation coefficients at 514.5- and 488.0-nm excitation were found to be 0.999 95 and 0.999 97 (for rhodamine 6G) and 0.999 99 and 0.999 99 (for rhodamine B) for the concentration range of 1.02×10^{-8} to 1.02×10^{-6} M. Four different mixtures of the two dyes having different relative concentrations were prepared. Using the method described in the theory section, the concentrations of each component in the mixtures were calculated from the measured fluorescence intensities at 514.5- and 488.0-nm excitation. The obtained concentrations are listed in Table III together with the added concentrations. In all cases and for concentrations of each component ranging from 5.1×10^{-9} to 5.1×10^{-8} M, good agreement was found between the added concentration and the calculated values.

Table III. Simultaneous Determination of Rhodamine B and Rhodamine 6G by AOTF-Based Fluorescence Spectrometry

	added		found	
sample no.	rhodamine B $\times 10^8$ M	rhodamine 6G $\times 10^8$ M	rhodamine B $\times 10^8$ M	rhodamine 6G $\times 10^8$ M
1	0.51	1.30	0.56	1.27
2	1.30	2.55	1.37	2.52
3	3.85	5.10	3.89	4.93
4	5.10	3.85	5.59	3.56

CONCLUSIONS

We have successfully demonstrated that it is possible to diffract light with more than one wavelength from the AOTF by simultaneously applying more than one rf signals into the filter. In this way, the AOTF behaves as a polychromator. This electronic polychromator inherently has more advantages compared to the conventional polychromators. As an example, each wavelength of the diffracted light can be readily and individually amplitude modulated at different frequency by individually and sinusoidally modulating each applied rf signal at the desired frequency. This feature makes this electronic polychromator uniquely suited for the development of a novel multidimension fluorescence spectrophotometer. A novel AOTF-based multidimension fluorimeter was successfully developed in which the sample was simultaneously excited by two different wavelengths whose amplitudes were modulated at two different frequencies. This fluorimeter was used for the determination of a sample having two different components. It should be noted that the objective of the present work is to demonstrate the principle and feasibility of the technique. Therefore, only two different rf signals (and hence two different wavelengths) were used. In principle, the AOTF can have truly multiwavelength capability. This is based on the fact that the total number of wavelengths of the diffracted light is determined by the total power of the applied rf for which the AOTF can tolerate. For this particular AOTF, the maximum rf power is 200 mW. Since each applied rf used in this work has a power of 20 mW, up to 10 different rf signals can be simultaneously applied, and hence, up to 10 different wavelengths can be diffracted from the filter. Higher rf power can be applied to a filter when it is specially constructed to exploit the resonance acoustic feature. In this study, a laser was used as the light source. However, the use of the AOTF is not restricted to this source. This is because the AOTF is known to have a relatively large acceptance angle compared to conventional

acousto-optic deflectors based on Bragg cells. In fact, it has been reported that an acceptance angle as large as 28° was achieved for AOTF.[18] As a consequence, the filter can be used for other light sources which do not provide low-diverging, well-collimated beams, e.g., incandescent and arc lamp. Furthermore, in the present work the AOTF is used only for the selection of the excitation wavelengths. A conventional monochromator was still utilized for the dispersion of the emission wavelengths. Advantages of the AOTF-based multidimension fluorescence spectrophotometer can, therefore, be fully achieved when (1) a continuous light source is used for excitation; (2) the emission monochromator is replaced with an AOTF; and (3) multi-rf signals are applied to both excitation and emission AOTFs. These are the subject of our intense investigation.

ACKNOWLEDGMENT

We are grateful to the National Institutes of Health, National Center for Research Resources, Biomedical Research Technology, for financial support of this work.

APPENDIX

Theory of Modulation and Data Analysis. The AOTF will diffract light with one wavelength when it is applied by a rf signal. The wavelength of the light diffracted from the AOTF is a function of the frequency of the rf signal. Increasing the frequency of the rf signal decreases the wavelength of the diffracted light. The efficiency of the diffraction is proportional to the power of the rf signal (e.g., for powers less than 20 mW for the AOTF used in this work). The wavelength and the intensity of the diffracted light can, therefore, be controlled by controlling the frequency and power of the applied rf signal, i.e.

$$I(\lambda_n) = I_o(\lambda_n)K(\lambda_n)P(\lambda_n) \quad (1)$$

where $I(\lambda_n)$ is the intensity of light of wavelength λ_n diffracted by the AOTF; $I_o(\lambda_n)$ is the intensity of the incident light at wavelength λ_n; $K(\lambda_n)$ is the proportional factor for wavelength λ_n; and $P(\lambda_n)$ is the power of the applied rf signal for wavelength λ_n.

If the applied rf signal is the mixture of different frequencies, i.e.

$$RF_{signal} = P_1 + P_2 + P_3 + ... + P_n \quad (2)$$

then the intensity of the light diffracted by the AOTF (I_{out}) is the sum of each individual signals $I_{\lambda_1}, I_{\lambda_2}, I_{\lambda_3}, ..., I_{\lambda_n}$, which correspond to the applied rf power P_1, P_2, P_3, ..., P_n, respectively.

$$I_{out} = I_{\lambda_1} + I_{\lambda_2} + I_{\lambda_3} + ... + I_{\lambda_n} \quad (3)$$

Furthermore, if the applied rf signal varies with time, the intensity of the diffracted light also varies

$$I_{out}(t) = I_{\lambda_1}(t) + I_{\lambda_2}(t) + I_{\lambda_3}(t) + ... + I_{\lambda_n}(t) \quad (4)$$

When the light $I_{\lambda_n}(t)$ whose intensity is a function of time (at a time scale much longer than the fluorescence lifetime of the compound) is used to excite a fluorescence sample having concentration c, the fluorescence intensity can be written as

$$F_{\lambda_n}(t) = L_{\lambda_n} I_{\lambda_n}(t) \quad (5)$$

where $L_{\lambda_n}(t)$ is proportional to the sample concentration and is dependent on the fluorescence properties of the sample.

(18) Katzka, P. *Proc. SPIE* **1987**, *752*, 23.

When the compound is simultaneously excited by more than one wavelength ($I_{\lambda_1}, I_{\lambda_2}, I_{\lambda_3}, ..., I_{\lambda_n}$), the fluorescence signal obtained (at one emission wavelength) is the sum of each signal induced by each excitation wavelength, i.e.

$$F(t) = F_{\lambda_1}(t) + F_{\lambda_2}(t) + F_{\lambda_3}(t) + ... + F_{\lambda_n}(t) \quad (6)$$

$$= L_{\lambda_1} I_{\lambda_1}(t) + L_{\lambda_2} I_{\lambda_2}(t) + L_{\lambda_3} I_{\lambda_3}(t) + ... + L_{\lambda_n \lambda_n}(t) \quad (7)$$

It will be demonstrated in the following section that by sinusoidally modulating the applied rf signal, the fluorescence signals, $F_{\lambda_1}(t)$, $F_{\lambda_2}(t)$, $F_{\lambda_3}(t)$, ..., induced by each excitation beam $I_{\lambda_1}(t), I_{\lambda_2}(t), I_{\lambda_3}(t), ...$, can be extracted from the measured total fluorescence $F(t)$.

To enable the AOTF to diffract light at wavelength λ_n, an rf signal with frequency f_n is needed

$$RF_n(t) = V_{no} \sin (2\pi f_n t) \quad (8)$$

The amplitude of this rf signal is sinusoidally modulated at frequency ω_n. The modulation sine wave is supplied by the computer and has the form

$$M_n(t) = 1 + m_n \sin (\omega_n t) \quad (9)$$

where m_n is the modulation index and ω_n is the angular frequency.

Upon amplitude modulation by this sine wave, the rf signal becomes

$$V_n(t) = V_{no} M_n(t) \sin (2\pi f_n t) \quad (10)$$

The diffraction efficiency of the AOTF is known to be proportional not to the intensity of the rf signal (in volts) but rather to the power of the rf signal.

Assuming that the change in the diffraction of the AOTF induced by the frequency of side bands generated by this sinusoidal modulation is very small and when $f_n \gg \omega_n/2\pi$, the averaged rf power in one cycle is approximated as

$$P_n(t) = P_{no}[M_n(t)]^2 \quad (11)$$

where $P_{no} = V_{no}^2/2R$; R is the impedance of the AOTF.

$$P_n(t) = P_{no}(1 + m_n \sin (\omega_n t))^2 =$$
$$P_{no}(1 + m_n^2/2) + 2m_n \sin (\omega_n t) - m_n^2/2 \cos (2\omega_n t) \quad (12)$$

When this modulated signal is applied to the AOTF, the diffracted light is modulated and its intensity is described as

$$I_{\lambda_n}(t) = I_{\lambda no}\{1 + m_n^2/2 + 2m_n \sin (\omega_n t) - m_n^2/2 \cos (2\omega_n t)\} \quad (13)$$

The average of this light intensity is

$$AV = \frac{1}{T}\int_t^{t+T} I_{\lambda_n}(t)\, dt = I_{\lambda_{no}}(1 + m_n^2/2) \quad (14)$$

where $T = 2\pi X_n/\omega_n$ and X_n is an integral number greater than 0.

The sinusoidally modulated component of the intensity is

$$Q_n = \frac{1}{T}\int_t^{t+T} I_{\lambda_n}(t) \sin (\omega_n t)\, dt = I_{\lambda_{no}} m_n \quad (15)$$

It is interesting to point out that there is no modulated component at frequencies other than ω_n and at wavelength other than λ_n. That is the value Q is zero for wavelength different from λ_n and for sinusoidal modulation $\omega \neq \omega_n$.

When more than one rf signal is simultaneously applied to the AOTF, the light intensity becomes

$$I(t) = I_{\lambda_1}(t) + I_{\lambda_2}(t) + ... + I_{\lambda_n}(t) \quad (16)$$

and the averaged component is

$$AV_1 = \frac{1}{T}\int_t^{t+T} I(t)\,dt = I_{\lambda 10}(1 + m_1^2/2) + I_{\lambda_{20}}(1 + m_2^2/2) + ... + I_{\lambda_{no}}(1 + m_n^2/2) \quad (17)$$

where

$$T = \frac{2\pi}{\omega_1}X_1 = \frac{2\pi}{\omega_2}X_2 = ... = \frac{2\pi}{\omega_n}X_n$$

where X_1, X_2, ..., X_n are lowest integral numbers (greater than 0).

The modulated component is

$$Q_{I_n} = \frac{1}{T}\int_t^{t+T} I(t)\sin(\omega_n t)\,dt = I_{\lambda_{no}} m_{no} \quad (18)$$

When this diffracted light is used to excite the sample, the corresponding averaged component of the fluorescence signal is

$$AV_F = \frac{1}{T}\int_t^{t+T} F(t)\,dt = L_{\lambda_1} I_{\lambda_{10}}(1 + m_1^2/2) + L_{\lambda_2} I_{\lambda_{20}}(1 + m_2^2/2) + ... + L_{\lambda_n} I_{\lambda_{no}}(1 + m_n^2/2) \quad (19)$$

and the modulated component is

$$Q_{F_n} = \frac{1}{T}\int_t^{t+T} F(t)\sin(\omega_n t)\,dt = L_{\lambda_n} I_{\lambda_{no}} m_{no} \quad (20)$$

The m_n and $I_{\lambda_{no}}$ values are known from the applied rf signals and the light source. The Q_{F_n} value can be determined by integrating the fluorescence signals as described in eq 20. From Q_{F_n}, $I_{\lambda_{no}}$, and m_n values, an L_{λ_n} value can be obtained. However, because the laser intensity, i.e., $I_{\lambda_{no}}$, can fluctuate with time, it is more accurate to determine L_{λ_n} from

$$L_{\lambda_n} = \frac{Q_{F_n}}{Q_{I_n}} \quad (21)$$

where Q_{F_n} and Q_{I_n} are obtained by integrating the fluorescence and excitation light intensity as described in eqs 20 and 18, respectively.

The L_{λ_n} value is proportional to the sample concentration C and is dependent on the fluorescence properties of the sample excited at wavelength λ_n.

Therefore

$$L_{\lambda_n} = l_{\lambda_n} C \quad (22)$$

where l_{λ_n} is constant which is independent of sample concentration and is dependent on the fluorescence of the sample excited at λ_n. Since each l_{λ_n} can be independently determined from calibration curves, sample concentration can be obtained from Q_{F_n} and Q_{I_n}.

The treatment can be extended for cases where the sample is a mixture of many components whose concentrations are C_1, C_2, ..., C_n. In this case

$$\begin{aligned} L_{\lambda_1} &= l_{\lambda_{11}} C_1 + l_{\lambda_{12}} C_2 + ... + l_{\lambda_{1n}} C_n \\ L_{\lambda_2} &= l_{\lambda_{21}} C_1 + l_{\lambda_{22}} C_2 + ... + l_{\lambda_{2n}} C_n \\ L_{\lambda_n} &= l_{\lambda_{n1}} C_1 + l_{\lambda_{n2}} C_2 + ... + l_{\lambda_{nm}} C_n \end{aligned} \quad (23)$$

Since L_{λ_1}, L_{λ_2}, and L_{λ_n} values are obtained from Q_{F_n} and Q_{I_n}, concentration for each componentcan be calculated.

RECEIVED for review May 20, 1992. Accepted August 20, 1992.